
LiBaGS: Lightweight Boundary Gap Synthesis for Targeted Synthetic Data Selection

Abhishek Moturu

Department of Computer Science
University of Toronto
The Hospital for Sick Children
UHN KITE Research Institute
T-CAIREM
Vector Institute
moturuab@cs.toronto.edu

Anna Goldenberg *

Department of Computer Science
Department of Laboratory Medicine and Pathobiology
University of Toronto
The Hospital for Sick Children
T-CAIREM
Vector Institute
anna.goldenberg@utoronto.ca

Babak Taati *

Department of Computer Science
Institute of Biomedical Engineering
University of Toronto
Rehabilitation Sciences Institute
UHN KITE Research Institute
Vector Institute
taati@cs.toronto.edu

Abstract

Synthetic data is useful only when the added samples fill missing parts of the training distribution that matter for the downstream task. We introduce **LiBaGS**, a lightweight, generator-agnostic method for targeted synthetic training data selection. LiBaGS scores candidate synthetic samples by combining decision-boundary proximity, predictive uncertainty, real-data density, and support validity, so that selected samples are both informative and likely to remain on the real data manifold. We then use a boundary-gap allocation rule that targets sparse but realistic decision-boundary neighborhoods, rather than simply adding more data or selecting only the most uncertain candidates. LiBaGS also learns when enough synthetic samples have been added through a marginal-value stopping rule, assigns softer labels near ambiguous boundaries, and uses a diversity objective to avoid redundant near-duplicate selections. Experiments show that LiBaGS improves accuracy over classical oversampling, hard augmentation, uncertainty-based selection, and targeted-generation selection criteria.

1 Introduction

Synthetic data has become a common way to improve supervised learning when real data is scarce, expensive, imbalanced, private, or locally incomplete. Classical oversampling methods such as SMOTE, Borderline-SMOTE, ADASYN, Safe-Level-SMOTE, KMeans-SMOTE, MWMOTE, and Geometric SMOTE generate synthetic samples by interpolating minority examples, emphasizing boundary-adjacent points, or changing the local sampling geometry [7, 14, 16, 6, 30, 4, 10]. Representation-space methods such as manifold oversampling and DeepSMOTE move this idea into learned features, which is especially relevant for image-like data [5, 9]. At the same time, augmentation methods such as mixup, Manifold Mixup, CutMix, Co-Mixup, CMO, and AugMax improve

*equal contribution

generalization by creating stronger or more diverse training examples [56, 48, 55, 23, 38, 49]. These methods show that synthetic or augmented data can help, but they also highlight a recurring issue: *not every synthetic sample is useful*.

This issue has become even more pronounced with modern generative models. GANs and diffusion models can produce large candidate pools, and recent work has shown that diffusion-generated data can improve image classification under the right conditions [12, 19, 3]. Targeted-generation methods go further by using uncertainty, classifier feedback, long-tail signals, hard-negative objectives, or curriculum schedules to generate more informative synthetic samples [37, 18, 26, 31, 2, 52, 32, 15, 24]. They show that useful synthetic data is often hard, uncertain, rare, or classifier-informative. But, many methods still treat usefulness primarily as a local score, a generation prompt, or a curriculum signal. LiBaGS instead asks a much more explicit allocation question: **where should synthetic samples be placed, and how many should be kept, after accounting for real-data coverage?**

A candidate can be rare but irrelevant if it lies far from the decision boundary. A candidate can be uncertain but redundant if the training set already contains many nearby samples. A candidate can look boundary-like but harmful if it is off the real data support. Useful targeted synthetic data should satisfy three conditions at once:

1. it should lie near a decision-boundary neighborhood,
2. occupy a region where real data is locally sparse, and
3. remain on support, i.e. resemble realistic data from the true distribution.

LiBaGS satisfies the above conditions. Let \mathcal{Z} denote the feature space, let $z \in \mathcal{Z}$ denote the feature representation of an input sample, $p(z)$ the real data density, $q(z)$ the synthetic allocation density, n the number of real samples, and m the number of synthetic samples. Let $r(z)$ be a local boundary-gap value that is high only when a candidate is boundary-relevant, uncertain, and support-valid.

We view classification error near the decision boundary as depending on how much useful data exists in a region. This can be approximated by:

$$J_m(q) = \int_{\mathcal{Z}} \frac{r(z)}{np(z) + mq(z)} dz. \quad (1)$$

Note that $np(z) + mq(z)$ represents the amount of local evidence from real and synthetic samples. Regions that already contain many real samples (large $p(z)$) benefit less from additional synthetic data. In contrast, regions with few real samples (small $p(z)$) but high boundary gap (large $r(z)$) is where synthetic samples can provide the greatest benefit.

Minimizing 1 gives the following boundary-gap allocation rule:

$$q^*(z) = \frac{1}{m} \left[\sqrt{\frac{r(z)}{\lambda} - np(z)} \right]_+, \quad (2)$$

where λ is a normalization constant automatically determined by the total synthetic allocation constraint. Intuitively, this rule places more synthetic samples in regions that are important for the decision boundary but poorly covered by real data, and places few or no synthetic samples in regions that already have enough real-data coverage.

LiBaGS is deliberately generator-agnostic and does not require retraining a diffusion model or training a new generator. A generator, interpolator, simulator, or augmentation pipeline proposes candidates, which LiBaGS then scores, filters, and diversifies. This is useful because generator quality varies. If a strong generator proposes many valid candidates, LiBaGS selects the most useful ones. If a weak generator proposes many artifacts, the support validity term and adaptive stopping rule prevent the method from blindly adding them. Thus, LiBaGS is a lightweight allocation rule that can be incorporated into existing synthetic data generating pipelines.

We make four contributions. First, we formulate targeted synthetic training data as a *boundary-gap allocation problem*. Second, we derive a boundary-gap allocation rule that uses boundary proximity, uncertainty, support validity, and real-density coverage. Third, we provide a practical finite-candidate algorithm with adaptive stopping and diversity-aware selection. Fourth, we empirically compare LiBaGS against classical oversampling, hard augmentation, uncertainty-based selection, and targeted-generation selection criteria. Full proofs are in Appendix A.

2 Related Work

Oversampling and interpolation. SMOTE and its variants are classical baselines for synthetic training data [7, 14, 16, 6, 30, 10, 4]. These methods are often framed around class imbalance, local minority neighborhoods, or interpolation geometry. LiBaGS is motivated by a related intuition that samples near the decision boundary are often especially useful. However, it differs in two important ways: it does not target boundary proximity alone but also discounts regions that are already well covered by real data and it is generator-agnostic and can select from any proposed synthetic candidate pool, rather than being limited to interpolation among minority-class examples.

Augmentation and mixing. Mixup, Manifold Mixup, CutMix, Co-Mixup, CMO, and AugMax improve generalization by creating similar, patch-level, context-rich, or hard augmented examples [56, 48, 55, 23, 38, 49]. These methods provide strong augmentation baselines, however, LiBaGS is complementary to them since it can select from augmented candidates by asking whether a candidate fills an under-covered decision-boundary neighborhood.

Targeted synthetic generation. TSynD optimizes latent representations toward high epistemic uncertainty for medical image classification [37]. Feedback-guided synthesis uses classifier feedback while emphasizing support and diversity [18]. GenDataAgent augments data on the fly using signals related to difficult training samples and gradient-update variance [31]. Deliberate Practice improves synthetic-data scaling by dynamically adding challenging examples [2]. DCDM and DisCL control sample difficulty or synthetic-to-real guidance levels [52, 32]. Longtail Guidance and Generate What Matters target rare, hard, or classifier-useful synthetic samples [15, 24]. Boundary-aware latent interpolation, on-manifold adversarial augmentation, targeted diffusion augmentation, and diffusion-based data augmentation are also related [33, 39, 36, 21, 53, 51]. But, LiBaGS contributes a density-aware allocation and stopping rule that can be applied after candidate generation.

Uncertainty, coverage, and active learning. Active learning selects informative real examples using uncertainty or coverage [42, 41]. Query synthesis and adversarial active sampling methods synthesize or search near decision boundaries rather than only sampling existing points [50, 34]. Training dynamics methods identify hard, ambiguous, or forgotten examples [46, 45]. LiBaGS synthetic selection also includes support filtering, since some generated candidates may fall outside the real data distribution and therefore be unrealistic or unhelpful for training.

3 Method

3.1 Setup and synthetic candidates

Let $\mathcal{D} = \{(x_i, y_i)\}_{i=1}^n$ be a supervised training set and let $h : \mathcal{X} \rightarrow \mathcal{Z}$ be a fixed representation map. A candidate generator produces:

$$\mathcal{C} = \{(\tilde{x}_j, \tilde{y}_j)\}_{j=1}^M, \quad z_j = h(\tilde{x}_j). \quad (3)$$

The generator can be a simulator, local interpolation rule, augmentation pipeline, autoencoder, diffusion model, or any class-conditioned sampler [25, 43, 12, 19, 21, 53, 51, 22]. LiBaGS only assumes access to the finite candidate pool. The goal is to select a subset $S \subseteq \mathcal{C}$ for final training.

For each candidate, LiBaGS estimates four quantities. First, a scoring model produces a class-probability vector $\pi(z)$, commonly used for predictive uncertainty, ensembles, and calibrated confidence scores in active learning / uncertainty estimation [42, 11, 29, 13]. The top-two margin is:

$$\Delta(z) = \pi_{(1)}(z) - \pi_{(2)}(z), \quad (4)$$

where smaller values indicate proximity to the decision boundary. To emphasize these boundary-adjacent regions, LiBaGS defines the smooth decision boundary neighborhood weight:

$$a_\tau(z) = \exp\left(-\frac{\Delta(z)^2}{2\tau^2}\right), \quad (5)$$

where $\tau > 0$ controls how broadly points are considered near the decision boundary, with small τ meaning narrow focus and large τ meaning broader boundary neighborhood. In practice, τ is

chosen from the empirical distribution of margin values (e.g., using a lower quantile of $\Delta(z)$ over the candidate pool), so that the weighting adapts to the amount of uncertainty in a given task.

The uncertainty score is the predictive entropy:

$$u(z) = H(\pi(z)). \quad (6)$$

The support-validity score $b(z) \in [0, 1]$ is high for candidates close to the real representation region, following the general idea that synthetic samples should remain near the real data support [18, 54]. The real-density estimate $\hat{p}(z)$ is computed using nearest-neighbor or kernel density estimates [8, 44]. The boundary-gap importance is then:

$$r(z) = a_\tau(z)u(z)b(z). \quad (7)$$

3.2 Boundary-gap allocation score

The continuous allocation rule in Eq. (1) leads to the following finite candidate score:

$$G_j = \left[\sqrt{\frac{r(z_j)}{\lambda}} - n\hat{p}(z_j) \right]_+. \quad (8)$$

Here, $r(z_j)$ measures how useful candidate z_j is for improving the decision boundary, while $\hat{p}(z_j)$ measures how well that region is already covered by real training data. The score therefore favors candidates that are both boundary-important and underrepresented in the real dataset.

Intuitively, G_j becomes large when a candidate lies in a high-uncertainty boundary region that still lacks sufficient real-data coverage, and becomes small when the candidate lies in a region that is already well covered, is far from the decision boundary, or appears off-support and therefore unlikely to provide useful training information.

3.3 Adaptive stopping

A fixed synthetic budget can be brittle, so LiBaGS instead uses an adaptive stopping rule related to diminishing-return selection and model-selection-by-stopping [20, 35, 27]. Intuitively, once a boundary region has already received enough synthetic coverage, adding additional nearby samples should provide progressively smaller gains.

Consider a local region of feature space with boundary importance r_j . Let c_j denote the amount of existing real-data coverage in that region, and let t_j denote the number of synthetic samples already allocated there. The marginal improvement from adding one more synthetic sample is modeled as:

$$\Delta_j(t_j) = \frac{r_j}{c_j + t_j} - \frac{r_j}{c_j + t_j + 1} = \frac{r_j}{(c_j + t_j)(c_j + t_j + 1)}. \quad (9)$$

As more synthetic samples are added to the same region, the marginal gain decreases. LiBaGS keeps adding candidates only while the best remaining marginal gain exceeds a threshold, $\eta > 0$, which is chosen from the flattening point of the ordered marginal gain curve. Thus, the number of selected synthetic samples $\hat{m} = |S|$ is learned from the candidate pool rather than fixed in advance.

3.4 Support filtering, soft labels, and diversity

A candidate with high uncertainty but a small support-validity score $b(z)$ is rejected unless it clears the stopping threshold. This is important when the generator is imperfect, since some boundary-like candidates may lie away from the real data support.

For labels, class-conditioned generators provide a proposed class $c(z)$. Near the boundary, hard labels can be overconfident, so we use the class-probability vector $\pi(z)$ to form a soft label:

$$\tilde{y}(z) = (1 - a_\tau(z))e_{c(z)} + a_\tau(z)\pi(z), \quad (10)$$

where $e_{c(z)}$ is the one-hot generator label and $\pi(z)$ is the class-probability vector from the scoring model. Further from the boundary, $a_\tau(z)$ is small, so the generator label is trusted more. Near the boundary, $a_\tau(z)$ is large, so the probability vector contributes more, reducing overconfidence in ambiguous regions.

Algorithm 1 Lightweight Boundary Gap Synthesis (LiBaGS)

Input: real training set \mathcal{D} , candidate generator, encoder h , scoring model

Output: final classifier, selected synthetic set S , and learned count \hat{m}

- 1: Train the scoring model on the real data only.
 - 2: Generate a candidate pool \mathcal{C} and map candidates to $z = h(x)$.
 - 3: For each candidate, estimate $\pi(z)$, $a_\tau(z)$, $u(z)$, $\hat{p}(z)$, and $b(z)$.
 - 4: Compute the boundary-gap allocation score G_j using Eq. (8).
 - 5: Compute candidate values $v_j = G_j b(z_j)$.
 - 6: Set the stopping threshold η using early stopping on marginal-gain curve.
 - 7: Select candidates greedily using Eq. (11) and stop when the best marginal gain is below η .
 - 8: Assign soft labels to selected candidates using Eq. (10).
 - 9: Train the final classifier on $\mathcal{D} \cup S$.
 - 10: **return** final classifier, selected synthetic set S , and $\hat{m} = |S|$.
-

Let $v_j = G_j b(z_j)$ and let $k(u, j)$ denote a similarity measure between candidates u and j in feature space, such as a Gaussian kernel or cosine similarity. For a selected set $S \subseteq \mathcal{C}$, LiBaGS maximizes:

$$F(S) = \sum_{u \in \mathcal{C}} v_u \max_{j \in S} k(u, j). \quad (11)$$

This objective rewards a selected set that covers many high-value candidates while avoiding redundant near-duplicates.

4 Theory

This section explains the main choices in Algorithm 1. The main idea is that useful synthetic candidates should be near the decision boundary, uncertain, supported by real data, diverse, and not already well covered by the real training set.

Theorem 1 (Local risk and boundary-gap allocation). *Assume that, in a small region around z , the local sample count is proportional to $np(z) + mq(z)$, where p is the real density and q is the selected synthetic density. If the local error decreases with this count and is weighted by this: $r(z) = a_\tau(z)u(z)b(z)$, then the allocation objective is:*

$$J_m(q) = \int_{\mathcal{Z}} \frac{r(z)}{np(z) + mq(z)} dz. \quad (12)$$

For fixed $m > 0$, for some $\lambda > 0$, minimizing $J_m(q)$ over $q \geq 0$ with $\int q(z) dz = 1$ gives:

$$q^*(z) = \frac{1}{m} \left[\sqrt{\frac{r(z)}{\lambda}} - np(z) \right]_+. \quad (13)$$

Proof sketch. Regions with larger $np(z) + mq(z)$ have lower local error, while regions with larger $r(z)$ are more important for boundary learning. The objective is convex in q and its optimal condition assigns synthetic mass until selected regions have equal marginal benefit. Subtracting the existing real coverage and clipping at zero gives Eq. (13); G_j in Eq. (8) is the finite-candidate version.

Theorem 2 (Adaptive stopping). *For a small region j , let $c_j > 0$ be real coverage, t_j the number of selected synthetic samples, and $r_j \geq 0$ the boundary importance. The gain of adding a sample is:*

$$\Delta_j(t_j) = \frac{r_j}{c_j + t_j} - \frac{r_j}{c_j + t_j + 1} = \frac{r_j}{(c_j + t_j)(c_j + t_j + 1)}. \quad (14)$$

Greedy selection with threshold η accepts gains $> \eta$ and stops when best remaining gain is $< \eta$.

Proof sketch. The gain $\Delta_j(t_j)$ decreases as t_j grows, so each region has diminishing returns. $\eta > 0$ is chosen from the flattening point of the ordered marginal gain curve. Greedy selection always takes the largest available gain and once that gain is below η , we stop.

Theorem 3 (Soft-label stability). *Let $\rho(z) = \Pr(Y | Z = z)$ be the true class distribution. The soft label $\tilde{y}(z) = (1 - a_\tau(z))e_{c(z)} + a_\tau(z)\pi(z)$ satisfies:*

$$\|\tilde{y}(z) - \rho(z)\|_1 \leq (1 - a_\tau(z))\|e_{c(z)} - \rho(z)\|_1 + a_\tau(z)\|\pi(z) - \rho(z)\|_1. \quad (15)$$

Proof sketch. The result follows directly from the triangle inequality applied to $\tilde{y}(z)$.

Theorem 4 (Diversity and support filtering). *Let $F(S) = \sum_{u \in \mathcal{C}} v_u \max_{j \in S} k(u, j)$ and let $v_u = G_u b(z_u)$, with $v_u \geq 0$ and $k(u, j) \geq 0$. Then, F is monotone submodular.*

Also, for a candidate j ,

$$F(S \cup \{j\}) - F(S) \leq \sum_{u \in \mathcal{C}} v_u k(u, j), \quad (16)$$

so candidates with low support-weighted neighborhood value cannot pass the stopping threshold.

Proof sketch. Adding a candidate can only increase coverage, so F is monotone. Adding a candidate also has diminishing returns, so F is submodular. Since $v_u = G_u b(z_u)$, low-support regions have small value and are filtered unless they still clear the marginal gain threshold.

5 Experiments

We evaluate LiBaGS in three settings: a two moons boundary-gap task, an 8×8 handwritten-digit 3 vs. 8 task, and a CIFAR-10 cat vs. dog image task. Across all experiments, LiBaGS uses the same procedure described in Section 3: a scoring model is trained only on the real training data, candidates are scored with $r(z) = a_\tau(z)u(z)b(z)$, the allocation score G_j is computed, candidates are selected by the objective with marginal-gain stopping, and selected candidates are assigned the soft label in Eq. (10). The selected synthetic count \hat{m} is learned independently on each seed and is not fixed in advance. For fair comparison, all fixed-count baselines receive the same learned synthetic count \hat{m} as LiBaGS on a given seed.

Datasets and setup. The two moons experiment is a nonlinear classification problem, where we draw real training points away from a central boundary region, so the training set contains a local coverage gap near the decision boundary. The candidate pool contains simulator-generated boundary candidates, additional supported candidates, and off-support candidates. The representation map h is a fixed random Fourier feature map, and the final classifier is logistic regression.

The 8×8 digits experiment uses the scikit-learn handwritten digits data [1], licensed under (CC BY 4.0), restricted to a binary 3 vs. 8 task (since these two numbers may have a difficult decision boundary). The real training set contains a small number of easy examples per class, while the candidate pool contains held-out hard digits, same-class interpolations, and low-structure digits. This setting tests whether LiBaGS can use the boundary-gap score to identify useful ambiguous candidates while avoiding off-support candidates.

For CIFAR-10 [28], which is widely used for research purposes, we use the cat vs. dog task with 25 real training images per class, 1000 auxiliary source images per class, and 800 test images per class. We use a frozen ResNet-50 [17] feature extractor from `timm`. The candidate pool is generated with Stable Diffusion v1-5 text/image-to-image model [40] using 50 candidates per class, diffusion strength 0.35, guidance scale 6.0, and 30 denoising steps. The generator is used only to produce the finite candidate pool; LiBaGS then selects a subset adaptively.

Baselines. We compare against empirical risk minimization (ERM) [47], random candidate selection, noise augmentation, and the same selection-signal baselines used in the CIFAR experiment: TSynD epistemic criterion [37], feedback-guided criterion [18], GenDataAgent gradient-variance criterion [31], Deliberate Practice entropy criterion [2], conformal filtering [54], long-tail rare/hard criterion [15], C2I boundary-influence criterion [24], and uncertainty-only [42]. On the two small datasets, we additionally include classical oversampling and augmentation baselines: SMOTE [7], Borderline-SMOTE [14], ADASYN [16], Safe-Level-SMOTE [6], KMeans-SMOTE [30], DeepSMOTE [9], and AugMax [49]. These additional baselines do not use the external candidate pool, but synthesize examples directly from the real training set.

Main results. Table 1 reports accuracy for the shared baselines across all three datasets. LiBaGS obtains the best mean accuracy in each setting. On two moons, LiBaGS improves over ERM from 0.8859 to 0.9454, showing that the boundary-gap allocation score recovers useful samples from the missing boundary region. On 8×8 digits 3 vs. 8, LiBaGS improves over ERM from 0.9391 to 0.9540, while also outperforming the other baselines. On CIFAR-10 cat vs. dog, LiBaGS reaches

Table 1: Accuracy across the three datasets across baselines used in the CIFAR-10 experiment. All non-ERM methods use the adaptive synthetic count learned by LiBaGS on each seed; means and standard deviations are over 5 seeds.

Method	Two moons	8x8 digits	CIFAR-10 cat/dog
ERM [47]	0.8859 \pm 0.0165	0.9391 \pm 0.0167	0.8040 \pm 0.0230
Noise augmentation	0.8977 \pm 0.0226	0.9342 \pm 0.0189	0.7918 \pm 0.0267
Random candidates	0.9299 \pm 0.0198	0.9491 \pm 0.0167	0.8120 \pm 0.0159
TSynD epistemic criterion [37]	0.9021 \pm 0.0313	0.9503 \pm 0.0158	0.8054 \pm 0.0173
Feedback-guided criterion [18]	0.9330 \pm 0.0184	0.9516 \pm 0.0265	0.8078 \pm 0.0158
GenDataAgent gradient-variance criterion [31]	0.9097 \pm 0.0840	0.9342 \pm 0.0306	0.8114 \pm 0.0150
Deliberate Practice entropy criterion [2]	0.9437 \pm 0.0169	0.9466 \pm 0.0303	0.8101 \pm 0.0140
Conformal filtering [54]	0.9209 \pm 0.0254	0.9466 \pm 0.0273	0.8130 \pm 0.0151
Long-tail rare/hard criterion [15]	0.9369 \pm 0.0197	0.9478 \pm 0.0143	0.8088 \pm 0.0167
C2I boundary-influence criterion [24]	0.9429 \pm 0.0170	0.9404 \pm 0.0222	0.8141 \pm 0.0149
Uncertainty-only [42]	0.9431 \pm 0.0166	0.9391 \pm 0.0178	0.8084 \pm 0.0199
LiBaGS	0.9454 \pm 0.0163	0.9540 \pm 0.0315	0.8159 \pm 0.0167

0.8159, compared with 0.8040 for ERM. These gains are modest but consistent, and they match the intended use case: LiBaGS is most useful when the candidate pool contains boundary-adjacent samples that are informative, on-support, and not already well covered by the real data. Together, the results suggest that explicitly targeting sparse boundary regions can improve synthetic-data selection without requiring a fixed (unknown) synthetic budget.

Tables 2 and 3 give the full results for the two moons experiment and the 8 \times 8 digits experiment, including the AUROC. The two moons experiment shows the largest absolute improvement because the missing boundary region is explicit. Figure 1 shows this explicitly. Although both tasks have several methods obtaining very similar ranking performance, LiBaGS is still the strongest on accuracy, while some uncertainty baselines have slightly higher AUROC. This suggests that LiBaGS is most useful as a targeted training-data selector: rather than simply improving global ranking of synthetic samples, it adds training signal in sparse boundary regions where additional examples can directly improve the learned classifier.

Table 2: Two moons results. LiBaGS learns the synthetic count (177.2 ± 42.5 across 5 seeds) by marginal-gain stopping; all baselines use this count for fair selection comparison.

Method	Accuracy	AUROC
ERM [47]	0.8859 \pm 0.0165	0.9554 \pm 0.0124
Noise augmentation	0.8977 \pm 0.0226	0.9626 \pm 0.0149
Random candidates	0.9299 \pm 0.0198	0.9800 \pm 0.0102
SMOTE [7]	0.8960 \pm 0.0197	0.9604 \pm 0.0152
Borderline-SMOTE [14]	0.9117 \pm 0.0212	0.9671 \pm 0.0145
ADASYN [16]	0.9083 \pm 0.0172	0.9652 \pm 0.0145
Safe-Level-SMOTE [6]	0.8939 \pm 0.0145	0.9584 \pm 0.0101
KMeans-SMOTE [30]	0.8957 \pm 0.0182	0.9598 \pm 0.0143
DeepSMOTE [9]	0.8967 \pm 0.0202	0.9601 \pm 0.0144
AugMax [49]	0.9086 \pm 0.0198	0.9660 \pm 0.0153
TSynD epistemic criterion [37]	0.9021 \pm 0.0313	0.9615 \pm 0.0239
Feedback-guided criterion [18]	0.9330 \pm 0.0184	0.9799 \pm 0.0137
GenDataAgent gradient-variance criterion [31]	0.9097 \pm 0.0840	0.9666 \pm 0.0475
Deliberate Practice entropy criterion [2]	0.9437 \pm 0.0169	0.9857 \pm 0.0083
Conformal filtering [54]	0.9209 \pm 0.0254	0.9725 \pm 0.0194
Long-tail rare/hard criterion [15]	0.9369 \pm 0.0197	0.9831 \pm 0.0112
C2I boundary-influence criterion [24]	0.9429 \pm 0.0170	0.9855 \pm 0.0080
Uncertainty-only [42]	0.9431 \pm 0.0166	0.9855 \pm 0.0083
LiBaGS (ours)	0.9454 \pm 0.0163	0.9853 \pm 0.0082

Table 3: 8×8 digits results on classes 3 vs. 8. LiBaGS learns the synthetic count (47.4 ± 10.2 across 5 seeds) by marginal-gain stopping; all baselines use this count for fair selection comparison.

Method	Accuracy	AUROC
ERM [47]	0.9391 ± 0.0167	0.9905 ± 0.0049
Noise augmentation	0.9342 ± 0.0189	0.9896 ± 0.0056
Random candidates	0.9491 ± 0.0167	0.9845 ± 0.0075
SMOTE [7]	0.9441 ± 0.0237	0.9915 ± 0.0059
Borderline-SMOTE [14]	0.9404 ± 0.0227	0.9895 ± 0.0065
ADASYN [16]	0.9478 ± 0.0209	0.9905 ± 0.0053
Safe-Level-SMOTE [6]	0.9453 ± 0.0221	0.9896 ± 0.0067
KMeans-SMOTE [30]	0.9453 ± 0.0161	0.9908 ± 0.0055
DeepSMOTE [9]	0.9366 ± 0.0217	0.9893 ± 0.0066
AugMax [49]	0.9404 ± 0.0251	0.9906 ± 0.0060
TSynD epistemic criterion [37]	0.9503 ± 0.0158	0.9859 ± 0.0080
Feedback-guided criterion [18]	0.9516 ± 0.0265	0.9860 ± 0.0203
GenDataAgent gradient-variance criterion [31]	0.9342 ± 0.0306	0.9845 ± 0.0106
Deliberate Practice entropy criterion [2]	0.9466 ± 0.0303	0.9911 ± 0.0072
Conformal filtering [54]	0.9466 ± 0.0273	0.9856 ± 0.0248
Long-tail rare/hard criterion [15]	0.9478 ± 0.0143	0.9914 ± 0.0063
C2I boundary-influence criterion [24]	0.9404 ± 0.0222	0.9904 ± 0.0065
Uncertainty-only [42]	0.9391 ± 0.0178	0.9917 ± 0.0051
LiBaGS (ours)	0.9540 ± 0.0315	0.9873 ± 0.0104

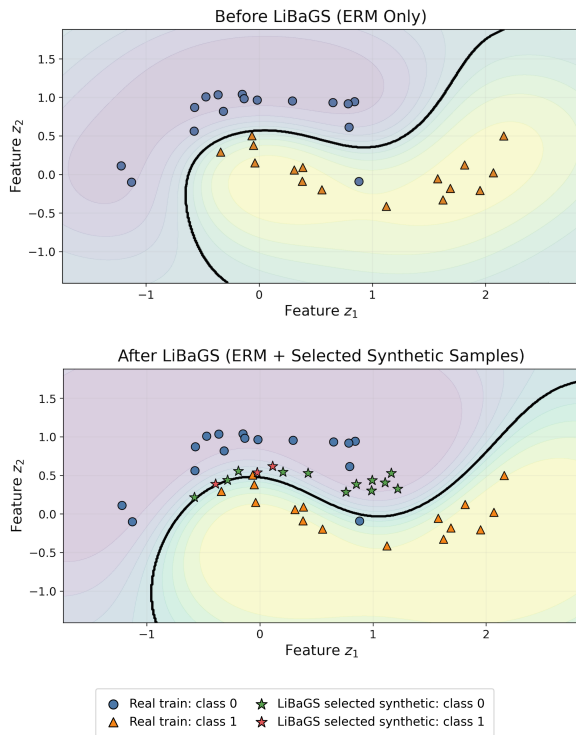


Figure 1: Qualitative illustration of boundary-gap selection on the two-moons task. **Top:** with only a small real training set, ERM learns an imperfect decision boundary because several boundary-neighborhood regions are weakly covered by real samples. **Bottom:** LiBaGS identifies synthetic candidates with high boundary-gap value, combining boundary proximity, uncertainty, support validity, and low real-data coverage. The selected candidates, shown as green and red stars, are added to the real training set and produce a visibly improved decision boundary. The background shading represents the predicted class-probability surface.

6 Computational cost

Let N be the number of real samples, M the number of synthetic candidates, and d the feature dimension. After candidate generation, LiBaGS has three main costs: fitting a lightweight scoring model on real features, scoring estimation for candidates, and diversity and support filtering, with the last step dominating the cost. The diversity and support filtering forms a candidate-candidate similarity matrix, costing $O(M^2d)$ time and $O(M^2)$ memory. Thus, after generation, the exact LiBaGS cost is $O(M^2d)$ for the asymptotic time complexity and $O(M^2)$ for the asymptotic space complexity. Empirically, for image data, generation still takes the most time and space. We used an NVIDIA A100 GPU with 40 GB of VRAM for the CIFAR-10 experiments, including image generation, which took about 1:20 minutes per seed run, given our run settings.

7 Discussion & Impact

LiBaGS can reduce the amount of real data needed in low-resource settings by selecting synthetic examples that target sparse boundary regions. This is especially useful when data collection is expensive, privacy-sensitive, time-consuming, or difficult to repeat. Rather than adding synthetic samples uniformly or relying only on uncertainty, LiBaGS attempts to identify candidates that are simultaneously near the decision boundary, plausible under the real data distribution, and located in regions with limited real-data coverage. This makes synthetic augmentation more targeted and can reduce unnecessary training on redundant or low-value generated samples.

The main risks come from synthetic data generation itself. If a generator reflects bias, label noise, spurious correlations, or unrealistic artifacts, LiBaGS may still select candidates that reinforce those problems. Support filtering reduces this risk but does not eliminate it, since a biased or incomplete real dataset can make biased synthetic samples appear on-support. Similarly, soft labels may reduce overconfidence near the boundary, but they cannot correct systematic errors in the generator or in the scoring model. As a result, LiBaGS should be viewed as a selection method rather than a guarantee of data quality.

In sensitive domains such as medicine, autonomous systems, education, etc., synthetic data can create a false sense of coverage. A selected synthetic sample may appear useful according to model-based scores while still being clinically implausible, demographically biased, or inconsistent with real deployment conditions. In such cases, LiBaGS should be paired with domain review, dataset audits, bias evaluation, external validation, and careful documentation of the generator, candidate pool, selected samples, and intended use.

8 Limitations

LiBaGS depends on the quality of the candidate pool. If the generator produces mostly easy examples, redundant examples, or off-support artifacts, the method may learn a small synthetic count or select candidates that provide only marginal gains. The method also relies on the representation map h and the scoring model; poor representations can make $\hat{p}(z)$, $b(z)$, and $\pi(z)$ unreliable. Future work should compare the baselines in large-scale or multi-class regimes. We also use selection-signal baselines rather than reproducing every full external pipeline, which isolates the relevant selection criteria but may not capture all implementation details of those methods in detail.

9 Conclusion

LiBaGS is a lightweight method for targeted synthetic data selection. Rather than adding a fixed number of generated samples, it scores candidates by boundary importance, uncertainty, support validity, and real-data coverage, then stops when the estimated marginal gain becomes small. Across the two moons task, the 8×8 digits 3 vs. 8 task, and the CIFAR-10 cat vs. dog experiment, LiBaGS improves over ERM and achieves the best mean accuracy among several selection baselines. The results support the claim that synthetic data is most useful when it fills sparse, on-support boundary gaps rather than merely increasing the size of the dataset.

References

- [1] E. Alpaydin and Fevzi. Alimoglu. Pen-Based Recognition of Handwritten Digits. UCI Machine Learning Repository, 1996. DOI: <https://doi.org/10.24432/C5MG6K>.
- [2] Reyhane Askari-Hemmat, Mohammad Pezeshki, Elvis Dohmatob, Florian Bordes, Pietro Astolfi, Melissa Hall, Jakob Verbeek, Michal Drozdal, and Adriana Romero-Soriano. Improving the scaling laws of synthetic data with deliberate practice. *arXiv preprint arXiv:2502.15588*, 2025.
- [3] Shekoofeh Azizi, Simon Kornblith, Chitwan Saharia, Mohammad Norouzi, and David J Fleet. Synthetic data from diffusion models improves imagenet classification. *arXiv preprint arXiv:2304.08466*, 2023.
- [4] Sukarna Barua, Md Monirul Islam, Xin Yao, and Kazuyuki Murase. Mwmote—majority weighted minority oversampling technique for imbalanced data set learning. *IEEE Transactions on knowledge and data engineering*, 26(2):405–425, 2012.
- [5] Colin Bellinger, Christopher Drummond, and Nathalie Japkowicz. Manifold-based synthetic oversampling with manifold conformance estimation. *Machine Learning*, 107(3):605–637, 2018.
- [6] Chumphol Bunkhumpornpat, Krung Sinapiromsaran, and Chidchanok Lursinsap. Safe-level-smote: Safe-level-synthetic minority over-sampling technique for handling the class imbalanced problem. In *Pacific-Asia conference on knowledge discovery and data mining*, pages 475–482. Springer, 2009.
- [7] Nitesh V Chawla, Kevin W Bowyer, Lawrence O Hall, and W Philip Kegelmeyer. Smote: synthetic minority over-sampling technique. *Journal of artificial intelligence research*, 16: 321–357, 2002.
- [8] Thomas Cover and Peter Hart. Nearest neighbor pattern classification. *IEEE transactions on information theory*, 13(1):21–27, 1967.
- [9] Damien Dablain, Bartosz Krawczyk, and Nitesh V Chawla. Deepsmote: Fusing deep learning and smote for imbalanced data. *IEEE transactions on neural networks and learning systems*, 34(9):6390–6404, 2022.
- [10] Georgios Douzas and Fernando Bacao. Geometric smote a geometrically enhanced drop-in replacement for smote. *Information sciences*, 501:118–135, 2019.
- [11] Yarín Gal and Zoubin Ghahramani. Dropout as a bayesian approximation: Representing model uncertainty in deep learning. In *international conference on machine learning*, pages 1050–1059. PMLR, 2016.
- [12] Ian J Goodfellow, Jean Pouget-Abadie, Mehdi Mirza, Bing Xu, David Warde-Farley, Sherjil Ozair, Aaron Courville, and Yoshua Bengio. Generative adversarial nets. *Advances in neural information processing systems*, 27, 2014.
- [13] Chuan Guo, Geoff Pleiss, Yu Sun, and Kilian Q Weinberger. On calibration of modern neural networks. In *International conference on machine learning*, pages 1321–1330. PMLR, 2017.
- [14] Hui Han, Wen-Yuan Wang, and Bing-Huan Mao. Borderline-smote: a new over-sampling method in imbalanced data sets learning. In *International conference on intelligent computing*, pages 878–887. Springer, 2005.
- [15] David S Hayden, Mao Ye, Timur Garipov, Gregory P Meyer, Carl Vondrick, Zhao Chen, Yuning Chai, Eric Wolff, and Siddhartha S Srinivasa. Generative data mining with longtail-guided diffusion. *arXiv preprint arXiv:2502.01980*, 2025.
- [16] Haibo He, Yang Bai, Eduardo A Garcia, and Shutao Li. Adasyn: Adaptive synthetic sampling approach for imbalanced learning. In *2008 IEEE international joint conference on neural networks (IEEE world congress on computational intelligence)*, pages 1322–1328. Ieee, 2008.

- [17] Kaiming He, Xiangyu Zhang, Shaoqing Ren, and Jian Sun. Deep residual learning for image recognition. In *Proceedings of the IEEE conference on computer vision and pattern recognition*, pages 770–778, 2016.
- [18] Reyhane Askari Hemmat, Mohammad Pezeshki, Florian Bordes, Michal Drozdal, and Adriana Romero-Soriano. Feedback-guided data synthesis for imbalanced classification. *arXiv preprint arXiv:2310.00158*, 2023.
- [19] Jonathan Ho, Ajay Jain, and Pieter Abbeel. Denoising diffusion probabilistic models. *Advances in neural information processing systems*, 33:6840–6851, 2020.
- [20] Wassily Hoeffding. Probability inequalities for sums of bounded random variables. *Journal of the American statistical association*, 58(301):13–30, 1963.
- [21] Khawar Islam, Muhammad Zaigham Zaheer, Arif Mahmood, and Karthik Nandakumar. Diffusemix: Label-preserving data augmentation with diffusion models. In *Proceedings of the IEEE/CVF Conference on Computer Vision and Pattern Recognition*, pages 27621–27630, 2024.
- [22] Jae Myung Kim, Jessica Bader, Stephan Alaniz, Cordelia Schmid, and Zeynep Akata. Datadream: Few-shot guided dataset generation. In *European Conference on Computer Vision*, pages 252–268. Springer, 2024.
- [23] Jang-Hyun Kim, Wonho Choo, Hosan Jeong, and Hyun Oh Song. Co-mixup: Saliency guided joint mixup with supermodular diversity. *arXiv preprint arXiv:2102.03065*, 2021.
- [24] Jeeyung Kim, Erfan Esmaeili, and Qiang Qiu. Generate what matters: Steering diffusion models for targeted data generation to improve classification. *OpenReview preprint*, 2025.
- [25] Diederik P Kingma and Max Welling. Auto-encoding variational bayes. *arXiv preprint arXiv:1312.6114*, 2013.
- [26] Soroush Abbasi Koohpayegani, Anuj Singh, KL Navaneet, Hamed Pirsiavash, and Hadi Jamali-Rad. Genie: Generative hard negative images through diffusion. *arXiv preprint arXiv:2312.02548*, 2023.
- [27] Andreas Krause and Daniel Golovin. Submodular function maximization. *Tractability*, 3(71-104):3, 2014.
- [28] Alex Krizhevsky, Vinod Nair, and Geoffrey Hinton. CIFAR-10 (Canadian Institute for Advanced Research), 2009.
- [29] Balaji Lakshminarayanan, Alexander Pritzel, and Charles Blundell. Simple and scalable predictive uncertainty estimation using deep ensembles. *Advances in neural information processing systems*, 30, 2017.
- [30] F Last, G Douzas, and F Bacao. Oversampling for imbalanced learning based on k-means and smote. *arXiv preprint arXiv:1711.00837*, 2, 2017.
- [31] Zhiteng Li, Lele Chen, Jerone Andrews, Yunhao Ba, Yulun Zhang, and Alice Xiang. Gendataagent: On-the-fly dataset augmentation with synthetic data. In *The Thirteenth International Conference on Learning Representations*, 2025.
- [32] Yijun Liang, Shweta Bhardwaj, and Tianyi Zhou. Diffusion curriculum: Synthetic-to-real data curriculum via image-guided diffusion. In *Proceedings of the IEEE/CVF International Conference on Computer Vision*, pages 1697–1707, 2025.
- [33] Kexin Liu, Hao Zhang, Yabin Wang, Chenxin Cai, Tingting Wu, and Jie Liu. Exploreaugment: Adaptive exploratory data augmentation based on boundary awareness. *OpenReview preprint*, 2025.
- [34] Christoph Mayer and Radu Timofte. Adversarial sampling for active learning. In *Proceedings of the IEEE/CVF winter conference on applications of computer vision*, pages 3071–3079, 2020.

- [35] George L Nemhauser, Laurence A Wolsey, and Marshall L Fisher. An analysis of approximations for maximizing submodular set functions—i. *Mathematical programming*, 14(1): 265–294, 1978.
- [36] Dang Nguyen, Jiping Li, Jinghao Zheng, and Baharan Mirzasoleiman. Do we need all the synthetic data? targeted synthetic image augmentation via diffusion models. *arXiv preprint arXiv:2505.21574*, 2025.
- [37] Joshua Niemeijer, Jan Ehrhardt, Hristina Uzunova, and Heinz Handels. Tsynd: Targeted synthetic data generation for enhanced medical image classification: Leveraging epistemic uncertainty to improve model performance. In *International Workshop on Simulation and Synthesis in Medical Imaging*, pages 69–78. Springer, 2024.
- [38] Seulki Park, Youngkyu Hong, Byeongho Heo, Sangdoon Yun, and Jin Young Choi. The majority can help the minority: Context-rich minority oversampling for long-tailed classification. In *Proceedings of the IEEE/CVF conference on computer vision and pattern recognition*, pages 6887–6896, 2022.
- [39] Kanil Patel, William Beluch, Dan Zhang, Michael Pfeiffer, and Bin Yang. On-manifold adversarial data augmentation improves uncertainty calibration. In *2020 25th International Conference on Pattern Recognition (ICPR)*, pages 8029–8036. IEEE, 2021.
- [40] Robin Rombach, Andreas Blattmann, Dominik Lorenz, Patrick Esser, and Björn Ommer. High-resolution image synthesis with latent diffusion models. In *Proceedings of the IEEE/CVF Conference on Computer Vision and Pattern Recognition (CVPR)*, pages 10684–10695, June 2022.
- [41] Ozan Sener and Silvio Savarese. Active learning for convolutional neural networks: A core-set approach. *arXiv preprint arXiv:1708.00489*, 2017.
- [42] Burr Settles. Active learning literature survey, 2009.
- [43] Connor Shorten and Taghi M Khoshgoftaar. A survey on image data augmentation for deep learning. *Journal of big data*, 6(1):1–48, 2019.
- [44] Bernard W Silverman. *Density estimation for statistics and data analysis*. Routledge, 2018.
- [45] Swabha Swayamdipta, Roy Schwartz, Nicholas Lourie, Yizhong Wang, Hannaneh Hajishirzi, Noah A Smith, and Yejin Choi. Dataset cartography: Mapping and diagnosing datasets with training dynamics. In *Proceedings of the 2020 Conference on Empirical Methods in Natural Language Processing (EMNLP)*, pages 9275–9293, 2020.
- [46] Mariya Toneva, Alessandro Sordoni, Remi Tachet des Combes, Adam Trischler, Yoshua Bengio, and Geoffrey J Gordon. An empirical study of example forgetting during deep neural network learning. *arXiv preprint arXiv:1812.05159*, 2018.
- [47] Vladimir N Vapnik. An overview of statistical learning theory. *IEEE transactions on neural networks*, 10(5):988–999, 1999.
- [48] Vikas Verma, Alex Lamb, Christopher Beckham, Amir Najafi, Ioannis Mitliagkas, David Lopez-Paz, and Yoshua Bengio. Manifold mixup: Better representations by interpolating hidden states. In *International conference on machine learning*, pages 6438–6447. PMLR, 2019.
- [49] Haotao Wang, Chaowei Xiao, Jean Kossaifi, Zhiding Yu, Anima Anandkumar, and Zhangyang Wang. Augmax: Adversarial composition of random augmentations for robust training. *Advances in neural information processing systems*, 34:237–250, 2021.
- [50] Liantao Wang, Xuelei Hu, Bo Yuan, and Jianfeng Lu. Active learning via query synthesis and nearest neighbour search. *Neurocomputing*, 147:426–434, 2015.
- [51] Yanghao Wang and Long Chen. Inversion circle interpolation: Diffusion-based image augmentation for data-scarce classification. In *Proceedings of the Computer Vision and Pattern Recognition Conference*, pages 25560–25569, 2025.

- [52] Zerun Wang, Jiafeng Mao, Xueting Wang, and Toshihiko Yamasaki. Training data synthesis with difficulty controlled diffusion model. *arXiv preprint arXiv:2411.18109*, pages 1–10, 2024.
- [53] Zhicai Wang, Longhui Wei, Tan Wang, Heyu Chen, Yanbin Hao, Xiang Wang, Xiangnan He, and Qi Tian. Enhance image classification via inter-class image mixup with diffusion model. In *Proceedings of the IEEE/CVF conference on computer vision and pattern recognition*, pages 17223–17233, 2024.
- [54] Zixuan Wu, So Won Jeong, Yating Liu, Yeo Jin Jung, and Claire Donnat. Filtering with confidence: When data augmentation meets conformal prediction. *arXiv preprint arXiv:2509.21479*, 2025.
- [55] Sangdoon Yun, Dongyoon Han, Seong Joon Oh, Sanghyuk Chun, Junsuk Choe, and Youngjoon Yoo. Cutmix: Regularization strategy to train strong classifiers with localizable features. In *Proceedings of the IEEE/CVF international conference on computer vision*, pages 6023–6032, 2019.
- [56] Hongyi Zhang, Moustapha Cisse, Yann N Dauphin, and David Lopez-Paz. mixup: Beyond empirical risk minimization. *arXiv preprint arXiv:1710.09412*, 2017.

A Technical appendices and supplementary material

A.1 Proof of Theorem 1

Theorem 1 (Local risk and boundary-gap allocation). *Assume that, in a small region around z , the local sample count is proportional to $np(z) + mq(z)$, where p is the real density and q is the selected synthetic density. If the local error decreases with this count and is weighted by this: $r(z) = a_\tau(z)u(z)b(z)$, then the allocation objective is:*

$$J_m(q) = \int_{\mathcal{Z}} \frac{r(z)}{np(z) + mq(z)} dz. \quad (17)$$

For fixed $m > 0$, for some $\lambda > 0$, minimizing $J_m(q)$ over $q \geq 0$ with $\int q(z) dz = 1$ gives:

$$q^*(z) = \frac{1}{m} \left[\sqrt{\frac{r(z)}{\lambda}} - np(z) \right]_+. \quad (18)$$

Proof. In a small region around z , the number of nearby training examples is proportional to $np(z) + mq(z)$. Local class-probability estimates become more stable as this count increases, so the local error is proportional to the inverse count. LiBaGS weights this local term using $r(z) = a_\tau(z)u(z)b(z)$, where $a_\tau(z)$ emphasizes boundary regions, $u(z)$ measures uncertainty, and $b(z)$ measures support. This gives the objective:

$$J_m(q) = \int_{\mathcal{Z}} \frac{r(z)}{np(z) + mq(z)} dz. \quad (19)$$

We optimize over valid synthetic allocation densities. The density $q(z)$ specifies where the fixed synthetic budget m is placed in representation space. Thus $q(z) \geq 0$ and $\int q(z) dz = 1$, while $mq(z)$ is the amount of synthetic mass assigned near z .

For a fixed z , define $\phi_z(q) = \frac{r(z)}{np(z) + mq}$. Since $\phi_z''(q) = \frac{2m^2 r(z)}{(np(z) + mq)^3} \geq 0$, each local term is convex in the allocation variable. Therefore, the full objective is convex in q .

Let q^* be the optimal allocation. A region with $q^*(z) > 0$ receives synthetic mass. Since the total synthetic budget is fixed, moving a small amount of mass between any two such regions should not reduce the objective; otherwise, q^* would not be optimal. The derivative $\frac{d}{dq(z)} \phi_z(q)$ measures local change from adding synthetic mass near z . It is negative because adding mass increases the denominator $np(z) + mq(z)$ and decreases the local objective term. If two selected regions had different derivatives, shifting mass toward the region with the larger decrease would improve allocation. So, all regions with $q^*(z) > 0$ must have the same derivative value. Hence, for some constant $C > 0$,

$$\frac{d}{dq(z)} \left(\frac{r(z)}{np(z) + mq(z)} \right) = -C. \quad (20)$$

Differentiating gives:

$$-\frac{mr(z)}{(np(z) + mq^*(z))^2} + C = 0. \quad (21)$$

Solving for the total local coverage gives:

$$np(z) + mq^*(z) = \sqrt{\frac{mr(z)}{C}}. \quad (22)$$

Absorbing constants into $\lambda = \frac{C}{m} > 0$ yields:

$$mq^*(z) = \sqrt{\frac{r(z)}{\lambda}} - np(z). \quad (23)$$

Since synthetic density cannot be negative, negative allocations are clipped to zero:

$$q^*(z) = \frac{1}{m} \left[\sqrt{\frac{r(z)}{\lambda}} - np(z) \right]_+, \quad (24)$$

where $\lambda > 0$ is chosen so that the allocation satisfies $\int q^*(z) dz = 1$.

Replacing z with z_j and replacing $p(z_j)$ with the empirical density estimate $\hat{p}(z_j)$ gives the finite-candidate score in Eq. (8). \square

A.2 Proof of Theorem 2

Theorem 2 (Adaptive stopping). *For a small region j , let $c_j > 0$ be real coverage, t_j the number of selected synthetic samples, and $r_j \geq 0$ the boundary importance. The gain from adding one more sample to region j is:*

$$\Delta_j(t_j) = \frac{r_j}{c_j + t_j} - \frac{r_j}{c_j + t_j + 1} = \frac{r_j}{(c_j + t_j)(c_j + t_j + 1)}. \quad (25)$$

Greedy selection with threshold η accepts gains $> \eta$ and stops when best remaining gain is $< \eta$.

Proof. For region j , adding one synthetic sample changes the local term from $\frac{r_j}{c_j + t_j}$ to $\frac{r_j}{c_j + t_j + 1}$. The gain is therefore:

$$\Delta_j(t_j) = \frac{r_j}{c_j + t_j} - \frac{r_j}{c_j + t_j + 1} = \frac{r_j}{(c_j + t_j)(c_j + t_j + 1)}. \quad (26)$$

As t_j increases, the denominator increases, so the marginal gain decreases. Thus, each region has diminishing returns: the first synthetic samples assigned to an under-covered region are more useful than later ones assigned to the same region.

With some threshold $\eta > 0$ (where η is chosen from the flattening point of the ordered marginal gain curve), adding a sample is worthwhile only if its gain is above η . Greedy selection always chooses the largest available gain across all regions. If this largest remaining gain is below η , then every other remaining gain is also below η , so no additional synthetic sample clears the stopping criterion.

Therefore, the greedy rule accepts exactly the samples whose estimated marginal gain is above η and stops once all remaining gains are too small. This proves the adaptive stopping rule and shows why the selected count \hat{m} is determined by the data rather than fixed in advance. \square

A.3 Proof of Theorem 3

Theorem 3 (Soft-label stability). *Let $\rho(z) = \Pr(Y | Z = z)$ be the true class distribution. The soft label $\tilde{y}(z) = (1 - a_\tau(z))e_{c(z)} + a_\tau(z)\pi(z)$ satisfies:*

$$\|\tilde{y}(z) - \rho(z)\|_1 \leq (1 - a_\tau(z))\|e_{c(z)} - \rho(z)\|_1 + a_\tau(z)\|\pi(z) - \rho(z)\|_1. \quad (27)$$

Proof. The soft label is:

$$\tilde{y}(z) = (1 - a_\tau(z))e_{c(z)} + a_\tau(z)\pi(z). \quad (28)$$

Subtracting the true class distribution $\rho(z)$ on both sides gives:

$$\tilde{y}(z) - \rho(z) = (1 - a_\tau(z))(e_{c(z)} - \rho(z)) + a_\tau(z)(\pi(z) - \rho(z)). \quad (29)$$

Taking the ℓ_1 norm and applying the triangle inequality, we get:

$$\|\tilde{y}(z) - \rho(z)\|_1 \leq (1 - a_\tau(z))\|e_{c(z)} - \rho(z)\|_1 + a_\tau(z)\|\pi(z) - \rho(z)\|_1. \quad (30)$$

\square

A.4 Proof of Theorem 4

Theorem 4 (Diversity and support filtering). *Let $F(S) = \sum_{u \in \mathcal{C}} v_u \max_{j \in S} k(u, j)$ and also let $v_u = G_u b(z_u)$, with $v_u \geq 0$ and $k(u, j) \geq 0$. Then, F is monotone submodular.*

Also, for a candidate j ,

$$F(S \cup \{j\}) - F(S) \leq \sum_{u \in \mathcal{C}} v_u k(u, j), \quad (31)$$

so candidates with low support-weighted neighborhood value cannot pass the stopping threshold.

Proof. Let $A \subseteq B$, then for every u ,

$$\max_{j \in A} k(u, j) \leq \max_{j \in B} k(u, j). \quad (32)$$

Since $v_u \geq 0$, summing over u gives $F(A) \leq F(B)$. Thus, F is monotone.

Let $A \subseteq B$ and $e \notin A, B$. For every u , let $m_A(u) = \max_{j \in A} k(u, j)$, $m_B(u) = \max_{j \in B} k(u, j)$.

Since $A \subseteq B$, we have $m_A(u) \leq m_B(u)$ for every u . The marginal gain of adding i to A is:

$$F(A \cup \{i\}) - F(A) = \sum_{u \in \mathcal{U}} v_u [\max\{m_A(u), k(u, i)\} - m_A(u)].$$

Equivalently,

$$F(A \cup \{i\}) - F(A) = \sum_{u \in \mathcal{U}} v_u [k(u, i) - m_A(u)]_+,$$

where $[x]_+$ clips negative values to 0. Similarly,

$$F(B \cup \{i\}) - F(B) = \sum_{u \in \mathcal{U}} v_u [k(u, i) - m_B(u)]_+.$$

Because $m_A(u) \leq m_B(u)$, we have:

$$[k(u, i) - m_A(u)]_+ \geq [k(u, i) - m_B(u)]_+$$

for every u . Since $v_u \geq 0$, summing over u gives:

$$F(A \cup \{i\}) - F(A) \geq F(B \cup \{i\}) - F(B).$$

Therefore, F is submodular.

So, F is monotone submodular, i.e. adding candidates always improves coverage, but each additional candidate gives increasingly smaller gains once similar candidates have already been selected.

Finally, the marginal gain of adding j , as also shown above, is:

$$F(S \cup \{j\}) - F(S) = \sum_{u \in \mathcal{C}} v_u \left[k(u, j) - \max_{\ell \in S} k(u, \ell) \right]_+. \quad (33)$$

Since $[x - y]_+ \leq x$ for $x \geq 0$,

$$F(S \cup \{j\}) - F(S) \leq \sum_{u \in \mathcal{C}} v_u k(u, j). \quad (34)$$

Thus, adding candidate j yields only a small gain when it is highly similar to candidates already contained in the selected set S . \square